Supplementary Material (ESI) for Chemical Communications

SUPPLEMENTARY DATA

Selectivity in small molecule binding to human telomeric RNA and DNA quadruplexes

Gavin Collie, Anthony P. Reszka, Shozeb M. Haider, Valérie Gabelica, Gary N. Parkinson & Stephen Neidle

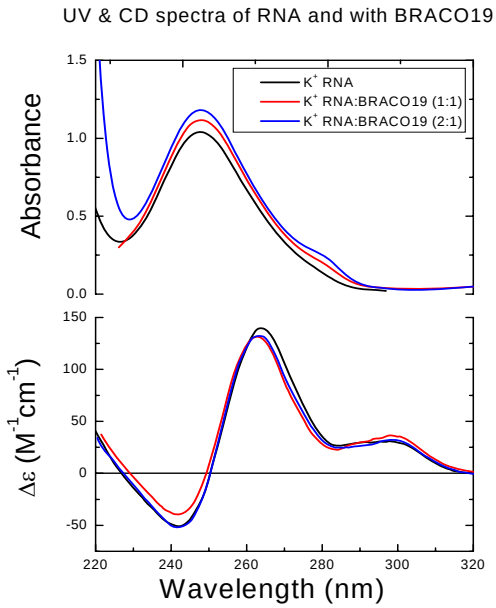

Supplementary Figure 1: Absorbance (top) and circular dichroism (bottom) spectra of the RNA quadruplex alone and titrated against BRACO-19, in K+ buffer, in 50 mM K^+ buffer

MOLECULAR DYNAMICS SIMULATION METHODS

The simulation protocols were consistent for all of the systems. Each systematic was equilibrated with explicit solvent molecules by 1000 steps of minimisation and 220ps of molecular dynamics at 300K. The entire systems were kept constrained, while allowing the ions and the solvent molecules to equilibrate. These systems were then subjected to a series of dynamics calculations in which the constraints were gradually relaxed, until no constraints at all were applied. The final production run was performed without any restrain on the complex for 20ns and co-ordinates were saved after every 10ps for analysis of the trajectories.

All calculations were carried out with the SANDER module of AMBER9.0 (www.ambermd.org), and with the SHAKE algorithm (Hauptman HA, Methods Enzymol, 1997, 277, 3-13) enabled for hydrogen atoms, with a tolerance of 0.0005A and a 2fs time step. The SHAKE feature constrains the vibrational stretching of hydrogen bond lengths and effectively fixes the bond distance to the equilibrium value. A 10 non-bonded Lennard-Jones cut-off was used and the non-bonded pairs list updated every 20steps. The Particle Mesh Ewal (PME) summation term was used for all simulations with the charge grid spacing at ~1.0 . The trajectories were analysed using the PTRAJ module available in AMBER9.0 suite and visualised by means of the VMD program (Humphrey W, Dalke A, Schulten K VMD - visual molecular dynamics. J Molec Graph 1996, 14, 33–38).

Free energies were calculated using the molecular mechanics, Poisson-Boltzmann and solvent-accessible surface area (MM-PBSA) method (Gilson MK and Honig B. 1998, Protein, 4:7-18). The electrostatic contribution to the solvation free energy was calculated using the Delphi program. Free energies were estimated by averaging the configurations that were collected at 20ps intervals for energetic analysis during the last 5ns of the MD simulation. This included the cations present within the electronegatively-charged central channel. These are considered to be an integral part of the structure and are required to be included in the MM-PBSA calculations in order to obtain meaningful results.

The AMBER parm99 charge set and Bondi radii (Bondi A. J. Phys. Chem, 1964, 68, 441-451) were
-2127).
All other calculations were carried out using internal scripts distributed with the AMBER 9.0 suite. The solute entropic contribution was estimated with the nmode program, using snapshots collected every 250ps.

All structural diagrams were prepared using the VMD program. All graphs were plotted using the Xmgrace program (http://plasma-gate.weizmann.ac.il/Grace/).

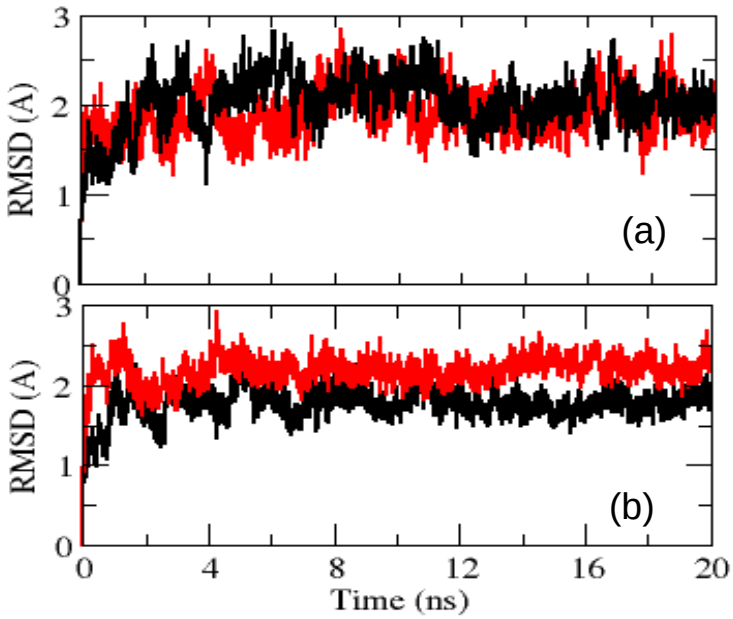

Supplementary Figure 2: The root mean square deviation (RMSD) plots comparing structural stability of the models over the course of the simulations. (a) The pattern of stability observed for 22-mer DNA (black) and RNA (red) quadruplexes is consistent with the thermodynamics and kinetic studies carried out by Mergny et al, with the RNA being more stable than DNA. (b) RMSD calculated from simulations of BRACO-19 complexed with DNA (black) and RNA (red) quadruplexes. The DNA quadruplex-drug complex is more stable than the RNA quadruplex-drug complex. The RMSD values are listed in table 1.

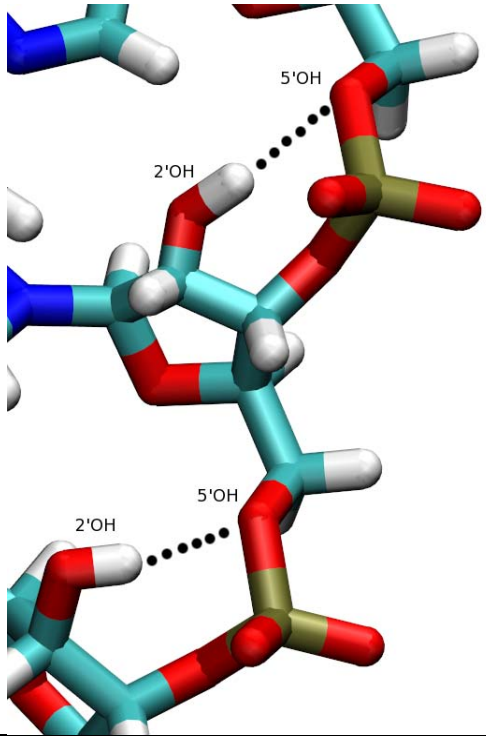

Supplementary Figure 3: Backbone interactions observed in the RNA quadruplex. Extra stability of the native 22-mer RNA quadruplex also comes from the sugar-phosphate backbone interactions. The 2'-OH group interacts with the 5'-OH group in the backbone, imparting rigidity to the structure.

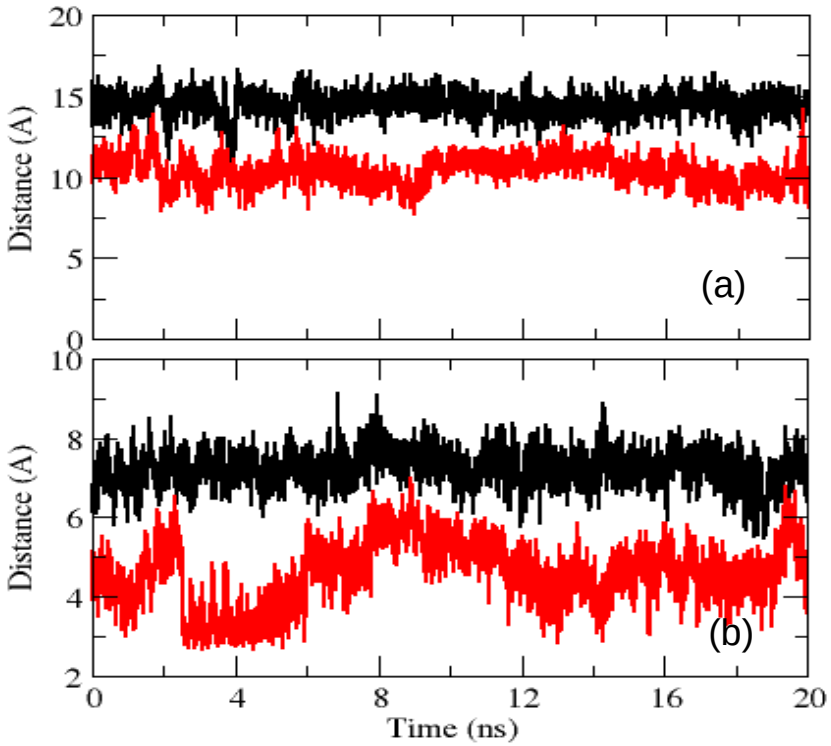

Supplementary Figure 4: Groove dimensions as calculated over the course of the 22mer DNA quadruplex (black) and 22-mer RNA quadruplex (red) simulations. The average groove depth (a) and width (b) corresponding to this graph has been listed in table 1. The groove dimensions are reduced by the presence of the 2'-OH group in RNA.

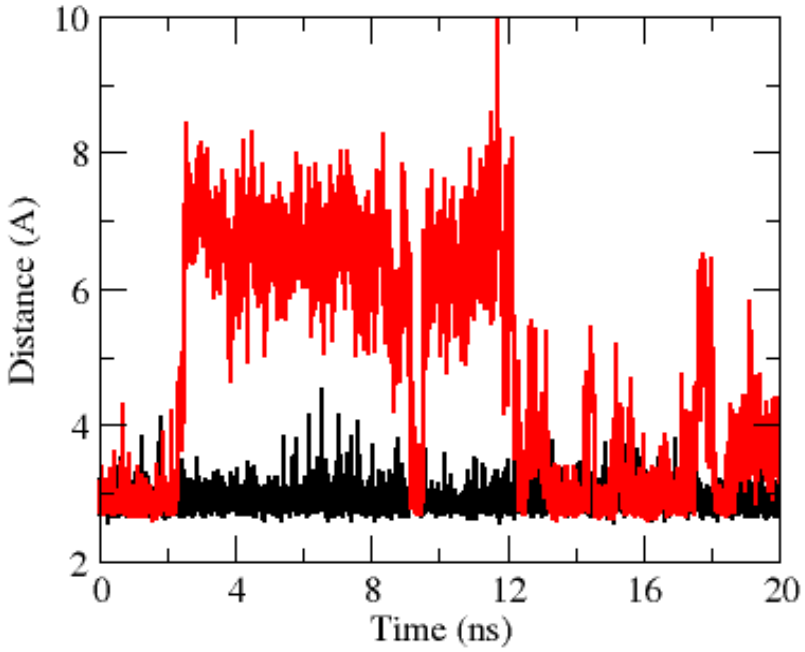

Supplementary Figure 5: Interactions between the amide nitrogen in BRACO-19 side chain with carbonyl oxygen from terminal thymine in the DNA quadruplex structure (black) and with carbonyl oxygen from terminal uracil in the RNA quadruplex complex. This interaction in the DNA quadruplex complex is extremely stable and is responsible for positioning the drug asymmetrically on one half of the quartet. The structural position of the 2'-OH group in guanine-17 in the RNA quadruplex complex is such that it is in close proximity of the amide carbonyl group. The repulsion between the two oxygens destabilises the interaction between the amide nitrogen and the carbonyl oxygen. As a consequence of this, the side chain oscillates thus further imparting instability to the structure.